

Document downloaded from:

<http://hdl.handle.net/10251/197962>

This paper must be cited as:

Cifuentes-Cabezas, MS.; Vincent Vela, MC.; Mendoza Roca, JA.; Alvarez Blanco, S. (2022). Use of ultrafiltration ceramic membranes as a first step treatment for olive oil washing wastewater. *Food and Bioprocesses*. 135:60-73.
<https://doi.org/10.1016/j.fbp.2022.07.002>



The final publication is available at

<https://doi.org/10.1016/j.fbp.2022.07.002>

Copyright Elsevier

Additional Information

Use of ultrafiltration ceramic membranes as a first step treatment for olive oil washing wastewater

Magdalena Cifuentes-Cabezas^{a*}, María Cinta Vincent-Vela^{a,b}, José Antonio Mendoza-Roca^{a,b} and Silvia Álvarez-Blanco^{a,b}

^a Research Institute for Industrial, Radiophysical and Environmental Safety (ISIRYM), Universitat Politècnica de València, C/Camino de Vera s/n, 46022, Valencia, Spain.

^b Department of Chemical and Nuclear Engineering, Universitat Politècnica de València, C/Camino de Vera s/n, 46022, Valencia, Spain

[*magdalena.cifuentesc@gmail.com](mailto:magdalena.cifuentesc@gmail.com) Address: Plaza José María Orense 8, d6, 46022, Valencia, Spain.

Abstract

Olive oil is a food product in great demand throughout the world, its production generating large volumes of wastewater with a high organic load, where phenolic compounds are present. These compounds have outstanding antioxidant characteristics, so their recovery is of great interest. In this way, the treatment of these wastewaters should be based on reusing water and, at the same time, on recovering valuable compounds. Ultrafiltration with ceramic membranes (5, 15 and 50 kDa) is proposed as a first treatment step for olive oil washing wastewater (OOWW) from the continuous two-phase centrifugation process. The effect of cross flow velocity and transmembrane pressure was evaluated against permeate flux values and the removal of turbidity, colour, chemical oxygen demand (COD), sugars and the phenolic compounds recovery. The CFV had a great influence on the removal of colour and turbidity. COD rejection increased with increasing TMP, being the highest rejection obtained under the most extreme conditions. The rejection of phenolic compounds and sugars did not show great variation between conditions. The 50 kDa membrane was the one that presented the largest permeate flux decline and the lowest permeability recovery after the cleaning, confirming the great fouling that this membrane suffered. The 15 kDa membrane at the operating conditions of $3 \text{ m}\cdot\text{s}^{-1}$ and 3 bar was observed as a good option to eliminate much of the colour (72%) and turbidity (99%) and to reduce considerably the organic load (54%) without greatly affecting the concentration of phenolic compounds (rejection of 21%) for future recovery.

Keywords: Ultrafiltration, ceramic membranes, olive oil washing wastewater, phenolic compounds, Industrial wastewater, Wastewater reuse

1. Introduction

Nowadays generation of wastewater is inevitable. The increasing demand for water, caused by the increase in economic activity, and the subsequent rapid industrial growth, has caused an abundant production of wastewater every year. Therefore, to face the threat of water scarcity, the purification or treatment of industrial wastewater is an essential factor to be considered (Mustafa et al., 2016).

These industrial activities generate wastewaters that vary significantly, with each industrial sector generating its own mix of pollutants. In the Mediterranean countries, one of the main sources of contamination is wastewater from olive oil mills (OMW), seasonally generated during the olive oil extraction process in the October-December season. Depending on the olive oil extraction methodology used, different wastewaters are generated. Of the three extraction processes (mechanical pressing, two-phase centrifugation and three-phase centrifugation), the centrifugation processes are the most widely used. These processes receive their name from the different phases that are obtained after the centrifugation of the olive paste to obtain olive oil. A horizontal decanter is used for this purpose. The three-phase centrifugation generates a solid waste, a raw olive oil and a wastewater; while the two-phase centrifugation process releases a wet solid phase and a raw olive oil. These two processes differ mainly in water consumption. Water is added in the three-phase process in the horizontal decanter unlike in the two-phase process (Núñez Camacho et al., 2021). The less amount of water used is the reason why two-phase centrifugation is considered a more ecological process than the three-phase centrifugation (Khdair and Abu-Rumman, 2020). In both processes, after the horizontal centrifugation, the raw oil is processed with a vertical centrifuge to remove residual water and solid particles, obtaining a clear virgin olive oil. Currently in Spain, the world's largest producer of olive oil in the world, the continuous two-phase centrifugation process is used in practically all the oil mills. Two types of wastewaters are generated in this centrifugation process: wastewater from olive washing (WOW) and wastewater from olive oil washing (OOWW) (Gebreyohannes et al., 2016).

Some studies have reported that WOW does not present an environmental problem (chemical oxygen demand (COD) $<1 \text{ g O}_2\cdot\text{L}^{-1}$) and can be used directly for irrigation or reused after a simple physical-chemical treatment. The case of OOWW is different, since it constitutes a serious environmental problem due to its high content of organic matter (COD between $3 \text{ gO}_2\cdot\text{L}^{-1}$ and $15 \text{ gO}_2\cdot\text{L}^{-1}$) (Maaitah et al., 2020). Apart from a high COD, another problem comes from the

presence of phenolic compounds, which have a negative effect on the biological treatment of OOWW. However, these compounds are widely known for their outstanding properties, such as anti-inflammatory, antimicrobial and antioxidant activity, inhibition of oxidative damage and elimination of free radicals, being highly valued by the pharmaceutical, cosmetic and food sectors (Garcia-Castello et al., 2010; Kaleh and Geißen, 2016).

Several alternatives have been considered for the treatment of OMW, such as physical, chemical and biological (aerobic and anaerobic) treatments and membrane processes (El-Abbassi et al., 2011). Membrane processes can be classified according to the driving force of separation. Among them, there are four processes where the driving force is provided by pressure. These can be classified according to the pore size distribution of the membrane and to the size of the retained substances. These processes are microfiltration (MF), ultrafiltration (UF), nanofiltration (NF), and reverse osmosis (RO). Membranes can also be grouped according to the materials used in their preparation (polymeric or ceramic membranes) (He et al., 2019). Polymeric membranes have been widely studied and they are mainly used in industrial water filtration processes. On the other hand, ceramic membranes have been studied in a limited way, due to several factors, one of the most important being the high manufacturing cost. However, in recent years, research on the applications of ceramic membranes in water treatment has attracted increased attention. This is due to the existing development, giving them greater mechanical, thermal and chemical stability, greater resistance to fouling and greater longevity of the membrane, favouring themselves to challenge water purification processes, such as textile wastewater treatment, oil-water separations and pharmaceutical wastewater treatment (Asif and Zhang, 2021; Li et al., 2020; Samaei et al., 2018). Although the use of ceramic membranes for the treatment of olive mill wastewater has already been studied (Paraskeva et al., 2007), most of the published works are focused on the use of these membranes in membrane bioreactor (MBR) systems (Değermenci et al., 2016; Dhaouadi and Marrot, 2008). In addition, in olive mills, unlike the wastewater produced in the three-phase centrifugation process, the effluent from the two-phase centrifugation process has been hardly studied. Of the three extraction processes (mechanical pressing, two-phase centrifugation and three-phase centrifugation), the centrifugation processes are the most widely used. These processes receive their name from the different phases that are obtained after the centrifugation of the olive paste to obtain olive oil. A horizontal decanter is used for this purpose. The three-phase centrifugation generates a solid waste, a raw olive oil and a wastewater; while the two-phase centrifugation process releases a wet solid phase and a raw olive oil. These two processes differ mainly in water consumption. Water is added in the three-phase process in the horizontal decanter unlike in the two-phase

process (Núñez Camacho et al., 2021). The less amount of water used is the reason why two-phase centrifugation is considered a more ecological process than the three-phase centrifugation (Khdaif and Abu-Rumman, 2020). In both processes, after the horizontal centrifugation, the raw oil is processed with a vertical centrifuge to remove residual water and solid particles, obtaining a clear virgin olive oil. Although the three-face process is the most widely used today, because the two-face process is more environmentally friendly, it is expected that the olive oil industry will adopt this production process in the future.

The main objective of this work was to evaluate the efficacy of ultrafiltration with ceramic membranes as a possible pre-treatment for a two-phase OOWW. For this, three Tami ceramic membranes with different molecular weights were tested in order to reduce the colour, turbidity, sugars and organic load of the wastewater, without significantly affecting the concentration of phenolic compounds in view of a future recovery of these compounds from the UF permeate. All membranes were tested under the same parameters, varying the cross flow velocity (CFV) and transmembrane pressure (TMP). There are very few studies carried out with ceramic membranes for the treatment of olive mill wastewater, the majority being with microfiltration membranes. On the other hand, almost all of the phenolic compound recovery works focus on wastewater from the three-phase process, with very few contemplating the two-phase process and none using ultrafiltration with ceramic membranes for this purpose. In addition, due to the numerous advantages of the two-phase process, especially from the environmental point of view, it will gain importance, which reinforces the interest of this work. Therefore, this study aims to expand the use of ceramic ultrafiltration membranes to remove the organic load from this type of wastewater.

2. Material and Methods

2.1 Wastewater samples

The wastewater samples correspond to olive oil washing wastewater (OOWW) obtained at the outlet of the vertical centrifuge in the continuous two-phase centrifugation process. The samples were provided by a Cooperative located in the Valencian Community in Spain. The samples were taken the same day and stored at -20°C, to avoid degradation.

2.2 Ultrafiltration procedure

Before the ultrafiltration stage, the effluents were pre-treated by flotation, sedimentation and filtration with a cartridge filter (60 µm), following the procedure explained in (Cifuentes-Cabezas et al., 2021). This treatment removes most of the larger particles, suspended solids and oils and

fats from the effluent, which can cause severe fouling of the membrane or damage to the ultrafiltration module and the plant.

The ultrafiltration experiments were carried out a laboratory-scale membrane plant (Orelis, France) (Fig. 1), where a tubular membrane module (Carbosep, Oreli Industriess, France) was installed. The experiments were carried out in full recycling filtration mode. Thus, the concentrate and permeate streams were continuously recirculated to the feed tank. Every 30 minutes, approximately 50 ml of permeate was collected for further analysis. A precision balance (Kern, Germany) was used to gravimetrically determine the permeate flux through the weight of the permeate. The measurements were recorded by a data acquisition system. During all the tests the temperature was kept constant around 25 °C (± 1) by means of a cooling jacket surrounding the feed vessel and a heat exchanger.

Table 1. Characteristic properties of the UF ceramic membranes tested in the experiments, manufacturer, literature and experimental data

INSIDE-CéRAM™ ultrafiltration membranes			
Support layer	TiO ₂	TiO ₂	TiO ₂
Active layer	TiO ₂ thin layer	ZrO ₂	ZrO ₂
MWCO ^a (kDa)	5	15	50
Pore size (nm)	2 – 4 ^b	-	8.6 ^c
T max (°C)	300	300	300
pH range	0 - 14	0 - 14	0 - 14
Contact angle (°)	40 ^d	43.8 ^e	42.4 ^e
Roughness (nm)	42 ^b	17.90 ^f	27.13 ^f
Permeability	>80 ^a	>80 ^a	>210 ^a
(Lh ⁻¹ m ⁻² bar ⁻¹)	97.38 ^h	100.37 ^h	220.77 ^h

^a: manufacturer data (Tami Industries, 2016); ^b: (Kujawa et al., 2016); ^c: (Lu et al., 2015); ^d: (Kujawa et al., 2020); ^e: (Urbanowska and Kabsch-Korbutowicz, 2021); ^f: (Corbatón-Báguena et al., 2014); ^g: Water at 25°C; ^h: Experimentally determined in this study

Three seven channel INSIDE CéRAM™ tubular ceramic membranes (Tami Industries, France) of different MWCO with an effective area of 132 cm² and 20 cm length were tested. The characteristics of these commercial membranes are shown in Table 1.

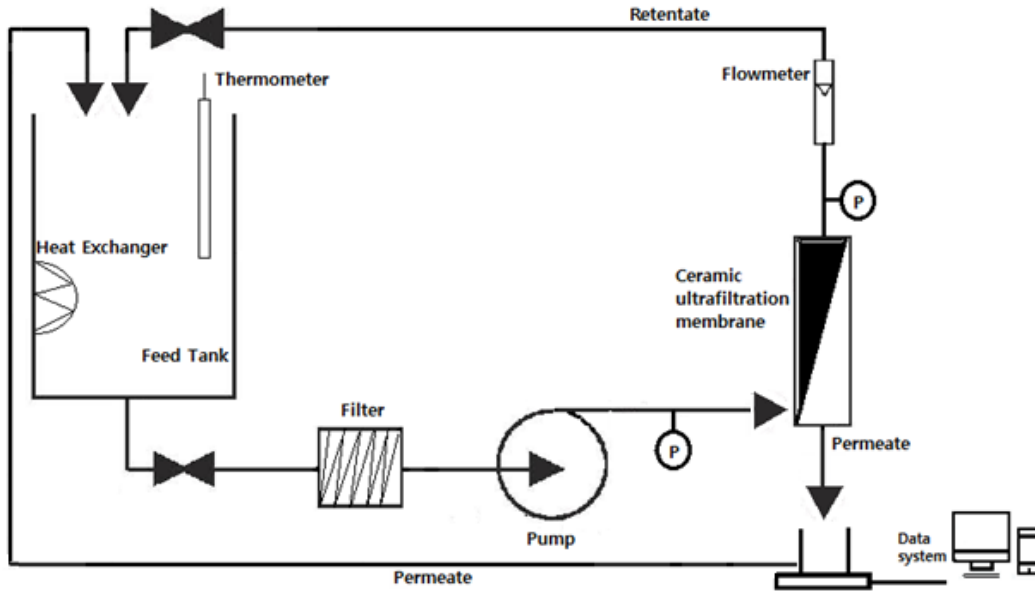


Fig. 1 Diagram of the ultrafiltration laboratory scale plant.

The aim was to study the evolution of the permeate flux over time as well as the rejection of colour, turbidity, COD, sugars and phenolic compounds, varying the crossflow velocity (CFV) and the transmembrane pressure (TMP). The CFV was varied between 2 and 4 m·s⁻¹ and the TMP between 1 and 3 bar. The duration of each test was 3 hours, which was enough time to reach the steady permeate flux. These operating conditions were selected to be comparable with other studies carried out with ultrafiltration membranes. Working ranges between 0.8 - 2.8 TPM and CFV of 3.9 - 5 ms⁻¹ have been reported for the treatment of olive mill wastewater with ceramic microfiltration and ultrafiltration membranes (Bottino et al., 2020; Değermenci et al., 2016; Paraskeva et al., 2007; Saf et al., 2022). On the other hand, similar ranges of operating conditions have been studied by other authors using the same membranes as in this study for the treatment of different wastewaters (Corbatón-Báguena et al., 2018; Luján-Facundo et al., 2016).

The efficiency of the membrane was evaluated by calculating the removal efficiency of colour and turbidity (Eq. 1) and the rejection of COD, sugars or phenolic compounds (Eq. 2).

$$E_i(\%) = \left(1 - \frac{V_{Pi}}{V_{Fi}}\right) \times 100 \quad (1)$$

$$R_j(\%) = \left(1 - \frac{C_{Pj}}{C_{Fj}}\right) \times 100 \quad (2)$$

Where E_i is the removal efficiency of parameter i (colour or turbidity) in %, V_{Pi} is the value of parameter i in the permeate stream, V_{Fi} is the value of parameter i in the feed solution, R_j is the rejection of parameter j (COD, sugars or phenolic compounds) in %, C_{Pj} is the concentration of

parameter j in the permeate stream and C_{Fj} is the concentration of parameter j in the feed solution.

After each experiment, the membranes were rinsed with tap water for 30 minutes. Then four cleaning protocols were proposed. Two of them were carried out with osmotic water varying the temperature (C_1 at 25 °C and C_2 at 35 °C). The other two protocols consisted of chemical cleaning using P3 Ultrasil 115 (Ecolab, Spain) at 1% v/v at different temperatures (C_3 at 25 °C and C_4 at 35 °C). This chemical was selected since its testified effect to reduce organic fouling (Luján-Facundo et al., 2016). All cleaning methods were carried out at $2 \text{ m}\cdot\text{s}^{-1}$, with a TMP of 0.5 bar for 40 minutes. Before and the cleaning, the membranes were rinsed with osmotic water and then the hydraulic permeability and verify the cleaning effectiveness. The hydraulic permeability (K) of all the membranes was calculated following the Darcy's equation (Eq. 3). Hydraulic permeability was determined with osmotized water at 25 °C, at TMPs of 0.5, 1, 2 and 3 bar.

$$J = K \cdot \Delta P = \frac{\Delta P}{\mu \cdot R_m} \quad (3)$$

With J representing the osmotic water permeate flux at a specific TMP (ΔP), μ the viscosity of the permeate and R_m the intrinsic membrane resistance. The membranes were considered to be clean if after the cleaning at least 90% of the initial osmotic water permeability was reached.

2.3 Analytical methods

A GLP 31+ conductivity-meter and a GLP 21+ pH-meter (Crison, Spain) were used for the conductivity and pH measurement, respectively. For the turbidity, the D-112 (DINKO, Spain) device was used following the UNE-EN ISO 7027 standard method. Colour (FZ) was calculated by spectral absorption coefficient (Döpkins et al, 2001), measuring the absorbances at 436, 525 and 620 nm with a DR600 spectrophotometer (Hach Lange, Germany). Anthrone colorimetric method (Frolund et al., 1996) was used for sugar content determination and Folin-Ciocalteu method (Singleton et al., 1999) for the measurement of total phenolic compounds concentration. Total suspended solids (TSS) were assessed following the UNE 77034 standard method (APHA, 2005). Oils and fats ($\text{mg}\cdot\text{L}^{-1}$) were measured by mass difference before and after an extraction process (modified Soxhlet protocol), and finally commercial kits (Merck, Germany) were used for COD measurement.

2.4 Particle size distribution

To evaluate the possible fragmentation of the particles present due to the turbulence generated on the membrane surface, it was decided to analyse the particle size distribution. For this, the feed samples were analysed before and after the experimental tests. The particle size

distribution was determined by Dynamic Light Scattering using the Zetasizer Nano ZS90 equipment (Malvern Instruments Ltd., UK).

3. Results and discussion

3.1 Characterization of OOWW samples

The main physicochemical characteristics of the raw and pre-treated OOWW (PR-OOWW) are shown in Table 2. In general, OMWs are slightly acidic, red to black coloured with high conductivity and organic matter concentration (Dermeche et al., 2013). In this case, the acidic profile (pH 5.09) and the high organic content (around $22 \text{ gO}_2\cdot\text{L}^{-1}$) were also observed. However, a yellow-green colour was predominant in the samples. Furthermore, their conductivity was not very high ($3.77 \pm 0.25 \text{ mS}\cdot\text{cm}^{-1}$). The samples presented a high concentration of total phenolic compounds (around $1.2 \text{ g Tyrosol eq}\cdot\text{L}^{-1}$). This was expected since OMWs are a good source of phenolic antioxidants (1–1.8% w/v), and according to Çelik et al. (2020) around 90% of the phenolic compounds presented in the olives are transferred to the wastewaters, obtained during the production process. This is due to the polar nature of oil mill wastewater compared to the non-polar nature of olive oil (Roselló-Soto et al., 2015).

The high concentration of TSS ($986.67 \pm 15.92 \text{ mg}\cdot\text{L}^{-1}$) and turbidity ($354 \pm 7.9 \text{ NTU}$) emphasizes the importance of a pre-treatment before the UF process for the removal of large particles that can severely damage both the membranes and the plant. Similar physicochemical characteristics were observed in other studies carried out by Ochando-Pulido et al. (2018, 2013). It is important to highlight that the composition of the OMWs not only depends on the olive oil extraction process, but it also changes with the variety of olive, the climatic conditions and the cultivation practices (Roig et al., 2006).

Table 2. Characterization results of raw (OOWW) and pre-treated (PR-OOWW) olive oil washing wastewater

Parameter	Raw OOWW	PR-OOWW
pH	5.09 ± 0.01	4.82 ± 0.01
Conductivity ($\text{mS}\cdot\text{cm}^{-1}$)	3.77 ± 0.25	3.44 ± 0.03
FZ ^a (colour)	4.30 ± 0.01	2.58 ± 0.01
Turbidity (NTU)	364.2 ± 7.9	211.6 ± 1.2
TSS ^b ($\text{mg}\cdot\text{L}^{-1}$)	986.67 ± 15.92	397.20 ± 9.09
Sugars ($\text{mgGlucose}\cdot\text{L}^{-1}$)	1645.32 ± 17.24	1334.75 ± 8.14
Oils and fats ($\text{mg}\cdot\text{L}^{-1}$)	308.15 ± 3.08	33.55 ± 0.81
Dissolved COD ^c ($\text{mgO}_2\cdot\text{L}^{-1}$)	23775.3 ± 238.2	17544.8 ± 220.6
TPhC ^d ($\text{mgTyrosol eq}\cdot\text{L}^{-1}$)	1161.80 ± 13.43	1103.80 ± 9.32

- ^a FZ: Farb-Zahl, colour measure
- ^b TSS: Total suspended solids.
- ^c COD: chemical oxygen demand
- ^d TPhC: Total phenolic compounds

Although the pre-treatment only decreased the content of organic matter (COD) by 26%, turbidity, colour and suspended solids concentration were reduced to a higher extent (around 40%). Regarding fats and oils, their elimination was very high, close to 90%. Their removal was very important as they have been demonstrated to have a great potential to foul the membranes (Tomczak and Gryta, 2020). The other parameters did not show great change, which is positive for the objective of the process, since the pre-treatment aimed to eliminate the largest organic particles, without affecting the concentration of phenolic compounds for their subsequent recovery.

3.2 Ultrafiltration: Hydraulic permeability of the membranes and permeate fluxes of the different conditions tested

The variation of permeate flux with TMP using osmotic water as feed for each membrane is shown in Fig. 2. By fitting osmotic water permeate flux against TMP, it was possible to calculate the hydraulic permeability for the membranes tested, according to Eq. 3. This parameter is characteristic of each membrane and was used to analyse the fouling produced when working with OOWW.

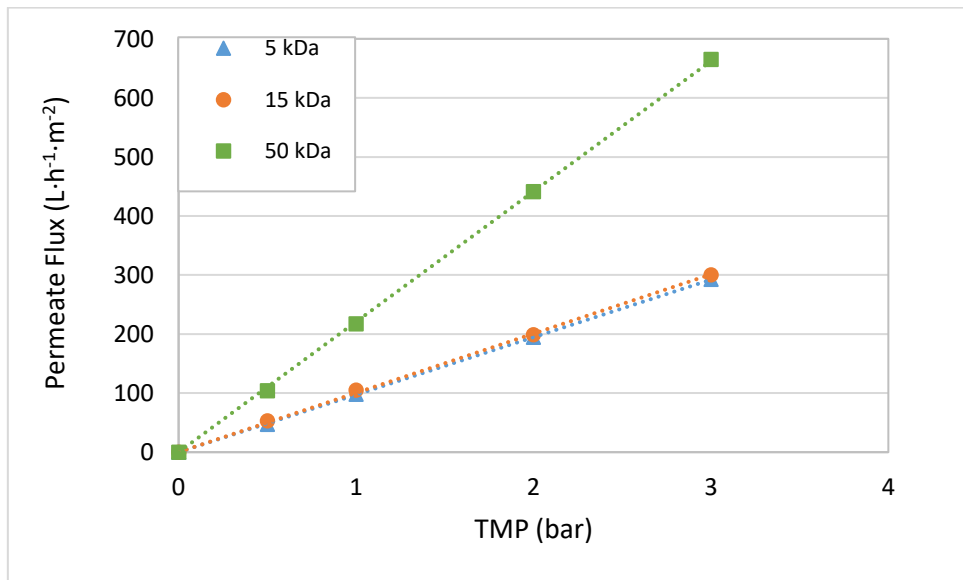


Fig. 2 Variation of permeate flux with transmembrane pressure for the different ultrafiltration membranes when osmotic water was used as feed (25 °C)

[Colour graph]

For the 5, 15 and 50 kDa MWCO membranes the hydraulic permeabilities were 97.38, 100.37 and 220.77 $\text{L}\cdot\text{m}^{-2}\cdot\text{h}^{-1}\cdot\text{bar}^{-1}$, respectively, with regression coefficients being higher than 0.998. According to the Hagen-Poiseuille equation, the value of the permeate flux must be proportional to the pore size of the membrane (Ahmed et al., 2017). However, in this case, the hydraulic permeability of the 15 kDa membrane was practically the same as that of 5 kDa one. This was not expected, but it is consistent with the information provided by the manufacturer (section 2.2). On the other hand, a similar phenomenon was also observed by other authors. Majewska-Nowak (2010) studied four ceramic membranes (also supplied by TAMI Industries) of different MWCO (1, 5, 8, and 15 kDa) for the separation of dyes. They pointed out that the permeability of these membranes did not show significant differences despite of their different MWCO, being the hydraulic permeability of the 1 kDa membrane greater than that of the 5 and 8 kDa membranes. This may mean that for, these Tami Inside ceramic membranes, pore size was not a key factor in the permeate flux value; and there are other factors that also influence the permeability of the membranes, such as surface porosity and the tortuosity of the pores.

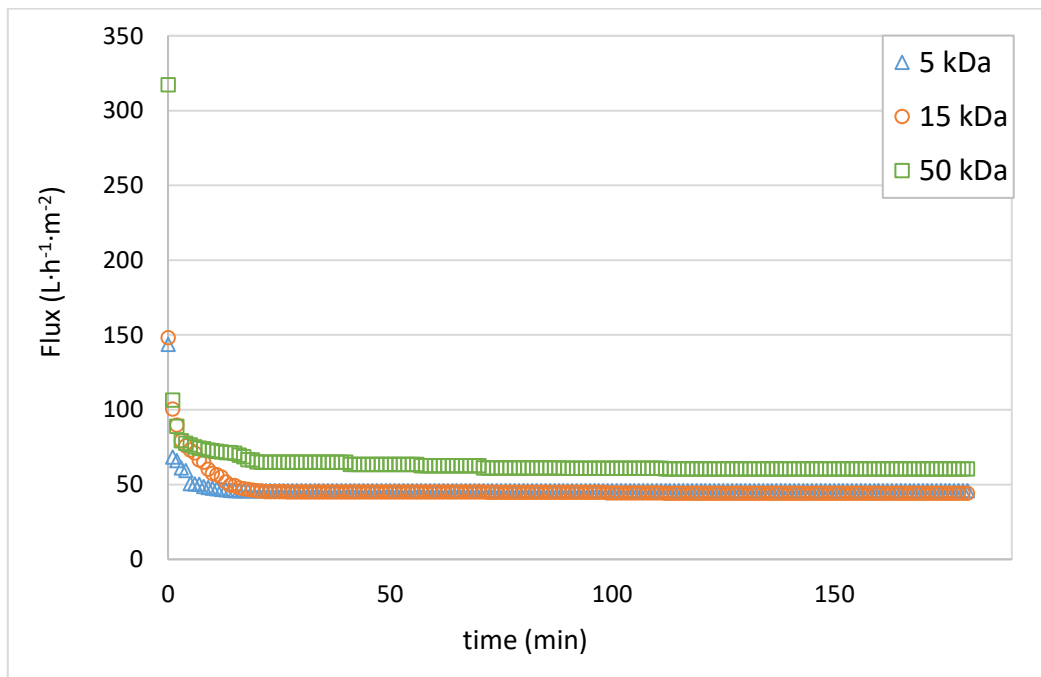


Fig. 3 Evolution of permeate flux with time for the tested ceramic membranes at a cross flow velocity of $3 \text{ m}\cdot\text{s}^{-1}$ and a transmembrane pressure of 1.5 bar (25°C) during pre-treated olive oil washing wastewater (PR-OOWW) ultrafiltration

[Colour graph]

Regarding the tests with OOWW, Fig. 3 shows permeate flux decline over time for the tests performed at $3 \text{ m}\cdot\text{s}^{-1}$ and 1.5 bar using PR-OOWW as feed. A sharp decrease in permeate flux was observed in the first minutes. After that sharp drop, there was a gradual but slow decrease

in permeate flux, reaching afterwards almost constant values. The same trend was observed for all the operating conditions considered. The decrease in permeate flux with time is mainly due to two phenomena: the accumulation and adsorption of molecules, gels and particles (fouling) on the surface of the membrane and inside the membrane pores and also an increase in the concentration of particles and solutes in a layer adjacent to the membrane surface due to convective transport, which causes concentration polarization phenomena, affecting the performance of the membrane (Tomczak, 2013). The 50 kDa membrane was the one that presented the greatest decrease in permeate flux in the first minutes (from 320 to 106 L·h⁻¹·m⁻² at the conditions considered in Fig. 3). This was observed in all the tests carried out, being more pronounced at the most extreme conditions (highest CFV and TMP). This can be related to the size of the membrane pores. As previously mentioned, the 50 kDa membrane presented the highest hydraulic permeability. Thus, the convective transport towards this membrane was expected to be the highest, generating a high concentration of solutes on the surface of the membrane. Moreover, this concentration polarization phenomenon favours fouling and gel layer formation, which also cause a flux drop over time. On the other hand, fouling is more severe when there difference between the MWCO of the membrane and the molecular weight of the solute molecules is small, as observed by several authors (Corbatón-Báguena et al., 2014; Luján-Facundo et al., 2016). Therefore, the large flux decay for the 50 kDa membrane may also be due to a blockage of the pores by substances with similar size to that of the membrane pores, which directly affects the selectivity of the membrane. This will be discussed again in section 3.3.

As in the case of the hydraulic permeability (Fig. 2), the 5 and 15 kDa membranes showed similar permeate flux values. This was observed for almost all tested operating conditions. Only under the operating conditions of 2 bar and 4 m·s⁻¹ the 5 kDa membrane presented higher but less stable fluxes compared to the 15 kDa membrane. The similar fluxes were also observed when steady permeate flux was plotted against TMP (Fig. 4). Then again, the 50 kDa membrane presented higher values of steady permeate flux due to its larger pore size and hydraulic permeability.

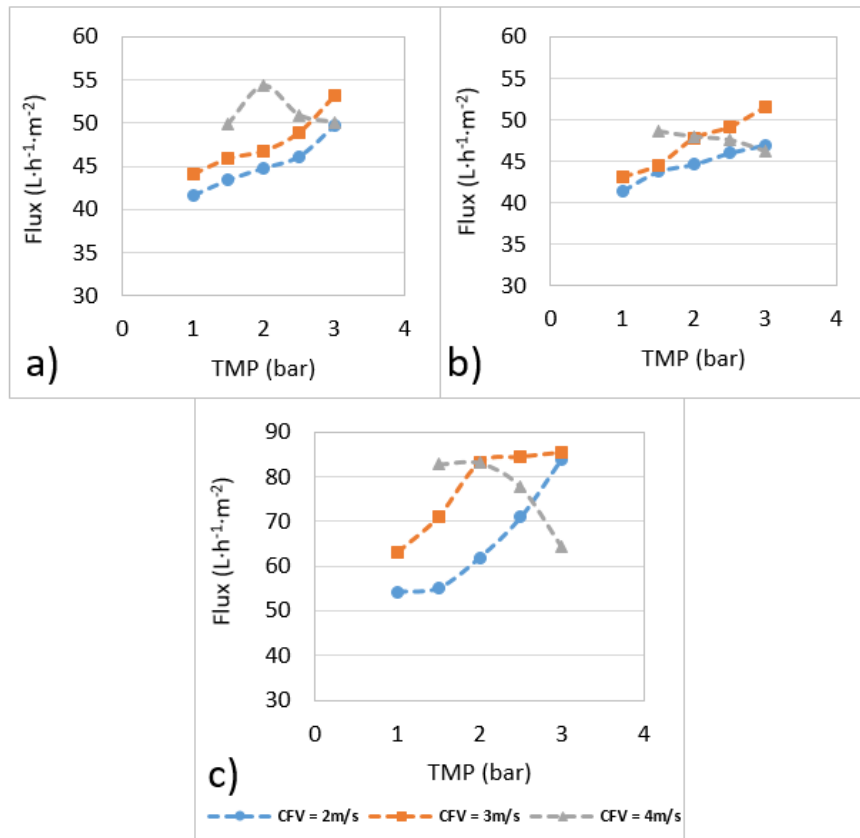


Fig. 4 Steady state permeate fluxes for the membranes tested at different operating conditions
 (a) 5 kDa; b) 15 kDa; c) 50 kDa)

[Colour graph]

According to the parameters evaluated, permeate flux increased slightly with TMP and CFV, the variation with CFV being greater for the membrane with the largest pore size. However, it can be seen in Fig. 4 that the variations with pressure are very small, sometimes even insignificant. This is because the limiting flux zone has been reached and therefore a gel layer has been formed on the surface of the membranes. For the highest CFV permeate flux showed a decrease with increasing TMP, especially in the case of the 50 kDa membrane. Ren et al. (2021) observed similar results when studying the best operating conditions for treating cattle wastewater with multichannel ceramic ultrafiltration membranes. They observed that the increase in both TMP and CFV generated an increase in the permeate flux until it reached the critical point. For TMP values above the critical point, permeate fluxes remained constant and even decreased. For the case of TMP, they stated that the decrease in flux might be due to the thickening and compression of the cake on the surface of the membrane, as well as to the distortion of the deposited particles. Concerning CFV, according to Foley et al. (1995) and Jepsen et al. (2018) as the CFV increases a reduction in the thickness of the cake is observed, however, smaller particles

are present in the layer. Therefore, the porosity of the cake decreases, which could generate a reduction in the flux. Jepsen et al. (2018) concluded that it is the ratio between the specific cake resistance and its thickness what can cause CFV to decrease the permeate flux. Therefore, higher rejections at the highest CFV were expected for the three membranes as a result of the compaction of the gel layer (This was confirmed from the experimental results shown in section 3.3). On the other hand, Tonova et al. (2020) also observed that permeate flux decreased with CFV under the presence of particles (flocs). These authors explained that the increase in CFV could cause a degradation of the particle size, which led to an improvement of the membrane fouling negatively affecting the flux. This can also be related to the fact that the suspended particles can break due to greater turbulence causing pore blocking, which is favoured by the increase in pressure. This implies an increase in the irreversible fouling.

To support this hypothesis, the particle size distribution of the feed samples used in the tests with the 50 kDa membrane were analysed. Samples before (initial) and after each test were characterized. It can be seen in Fig. 5 that the tests at 2 and 3 $\text{m}\cdot\text{s}^{-1}$ do not present a great variation in the particle size distribution when increasing the TMP from 1 to 3 bar. However, at 4 $\text{m}\cdot\text{s}^{-1}$ the pressure increase generated a notable decrease in particle size, reaching a mean particle size of 695.7 nm at the highest TMP tested when the initial average size was 1183 nm. It has to be mentioned that the measure of the particle size distribution was performed by dynamic light scattering. The measurement values are higher than the real values when particles of a wide range of sizes are found in a sample. This is due to fact that the equipment measures intensities of scattered light and larger particles hide the intensity scattered by the smaller ones. However, it is clear the diminution of the particle size in the feed for the highest cross-flow velocity.

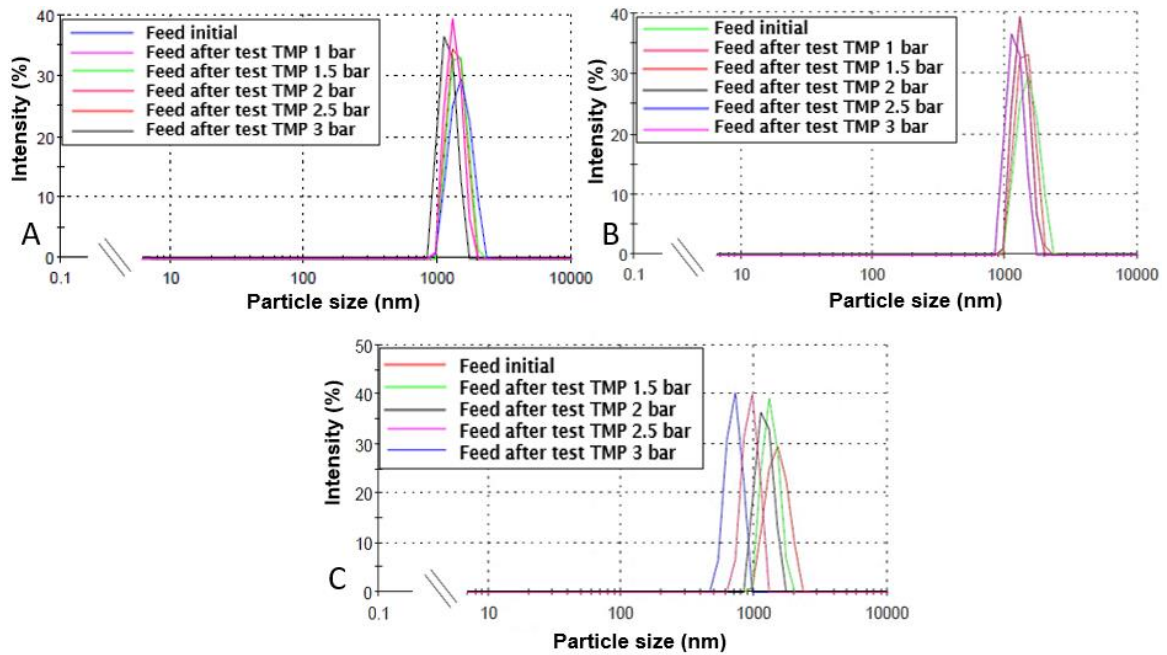


Fig.5 Feed particle size distribution for the ultrafiltration tests performed with the 50 kDa membrane

A: CFV of $2\text{ m}\cdot\text{s}^{-1}$; B: CFV of $3\text{ m}\cdot\text{s}^{-1}$; C: CFV of $4\text{ m}\cdot\text{s}^{-1}$

[Colour graph]

A reduction in the particle size of the feed with CFV was also observed by Ho and Sung (2009) in their work on the effect of solids concentration and CFV on anaerobic sludge microfiltration. They observed a decrease in the mean particle size of the anaerobic sludge from $56\text{ }\mu\text{m}$ (CFV of $0.1\text{ m}\cdot\text{s}^{-1}$) to $44\text{ }\mu\text{m}$ after 6 h of filtration at $0.7\text{ m}\cdot\text{s}^{-1}$. These authors explained that the particles in MBR broke down into finer particles due to the high shear stress, to later form a denser cake layer. The shear stress generated by the CFV showed a linear trend. Moreover, Du et al. (2019) reported that high CFV induced a higher shear stress by increasing the lifting force exerted on the particles, which could help large particles to move away from the membrane surface, causing small particles to settle on the membrane surface and cause severe fouling. That reason why this behaviour was observed for this membrane and not for the others may be due to the fact that pores with a larger diameter are more susceptible to internal obstruction by smaller particles (Waeger et al., 2010).

Finally, the trend observed in Fig. 4c, that is, the loss of the linear correlation of the permeate flux with the TMP, is due to the fact that this increase in pressure generates a compaction of the membrane or enhances the polarization of the concentration. This in turn produces an increase in transfer resistance; then the dependence of flow against pressure deviates significantly from

the linear trend and can exhibit a null trend (Fig 4c, test at 3 m·s⁻¹) or even negative trend (Fig 4c, test at 4 m·s⁻¹).

It is also important to note that flux values were considerably lower than those measured for osmotic water. This was observed for all the tested operating conditions and the difference was even more relevant for the membrane with the highest MWCO. This indicates a strong fouling of the membrane, which is generally attributed to solute adsorption, pore blocking and to the formation of a gel layer. The "fouling potential" of each membrane depends on the characteristics of the membrane surface and the wastewater (solute present) (Žabková et al., 2007). In this way, the fouling tendency of a membrane is related to the roughness of the active layer. The higher its roughness, the more susceptible the membrane is to fouling (Schäfer et al., 2000). This is explained because a rougher surface could favour the entrapment of solute molecules, forming a fouling layer which acts as a second barrier to separation (Garcia-Ivars et al., 2017). According to studies carried out by Corbatón-Báguena et al. (2014), the 50 kDa membrane has higher surface roughness than the 15 kDa membrane (root mean square roughness of 27.33 nm vs 17.90 nm, respectively). On the other hand, the pore size of the membrane and the molecular weight of the solute molecules present in the wastewater play an important role in fouling. If the sizes are similar, the membrane is more susceptible to pore blockage (Liu et al., 2020).

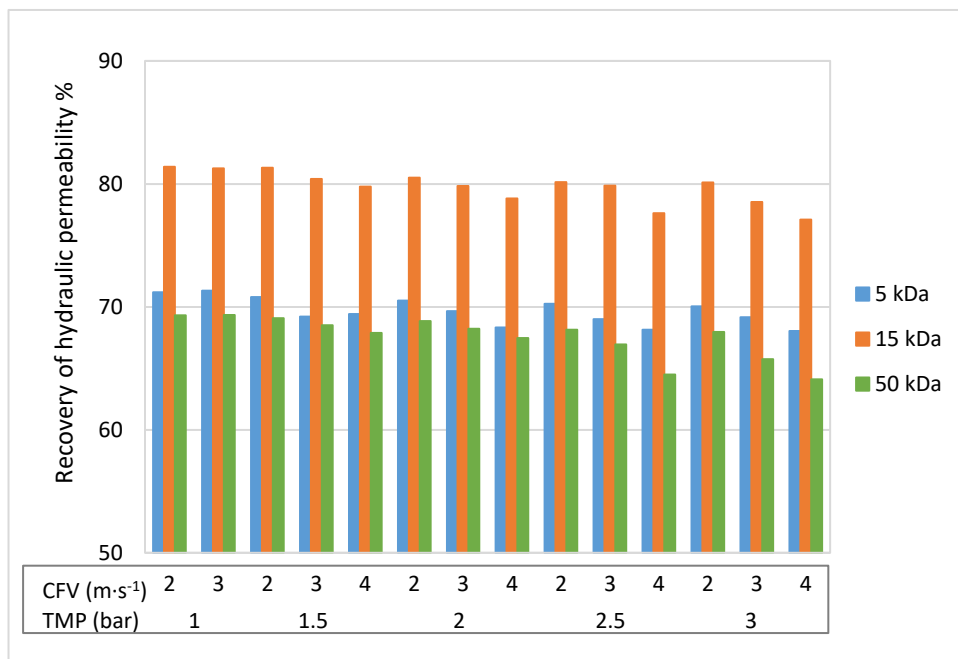


Fig. 6 Recovery of the hydraulic permeability of the ceramic ultrafiltration membranes by rinsing with osmotic water (25°C) after the tests performed at the different operating conditions

[Colour graph]

Fig. 6 corroborates what has been commented above. It shows the recovery of the hydraulic permeability of the membranes after rinsing with tap water followed by rinsing with osmotic water. It is observed that the higher the CFV and the TMP, the lower the recovery of the permeate flux, being more noticeable for the membrane with the highest MWCO. Therefore, irreversible fouling increases with increasing CFV and TMP above 1 bar. In addition, it can be also observed that the 50 kDa membrane exhibited the most severe fouling.

On the other hand, the 15 kDa membrane was the one that showed the highest percentage of permeability recovery (around 80%), corresponding therefore to the lowest irreversible fouling. This was observed in all the tests carried out at the different operating conditions. Interestingly, it can be noted that the membranes with higher and lower MWCO presented greater irreversible fouling.

Water rinsing removes the reversible membrane fouling, while the remaining fouling corresponds to the irreversible fouling of each membrane. To eliminate it, it would be necessary to use a chemical agent, as will be discussed in section 3.4.

3.3 Ultrafiltration: solute rejection

Fig. 7 shows turbidity (white) and colour (green) removal efficiencies, calculated according to equation (2). For the three membranes, the removal of turbidity increased with CFV and TMP. This was expected since the higher the CFV, the lower the concentration of solutes on the membrane surface. The percentages of turbidity removal were high, reaching in some cases values close to 99%. These high percentages are due to the fact that most of the solids that contributed to turbidity are larger than the pores of the membranes. In this way, UF membranes are able to almost completely eliminate turbidity regardless of the type of wastewater (Gao et al., 2011; Hube et al., 2020). Moreover, as expected, the 5 kDa membrane (the one with the lowest MWCO) achieved the greatest turbidity removal.

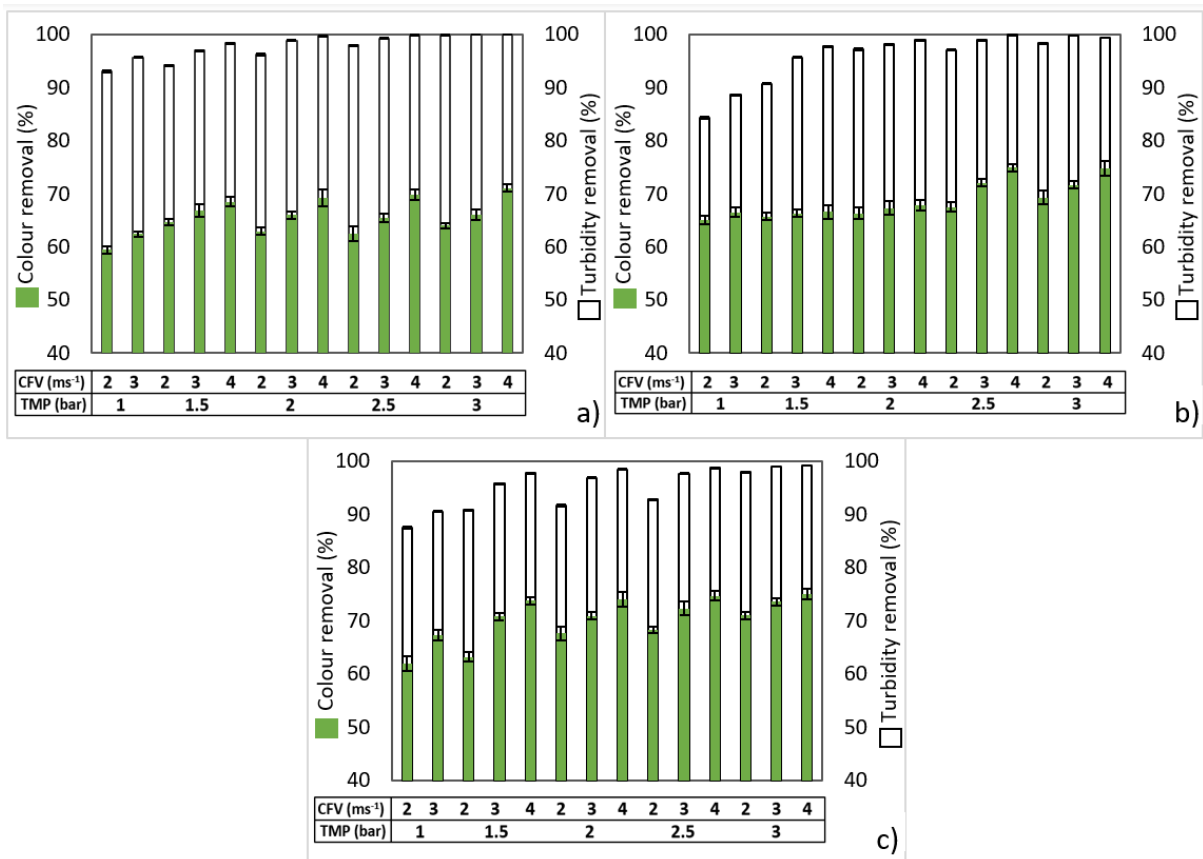


Fig. 7 Removal of Colour (green) and turbidity (white) for the different membranes and operating conditions; a) 5 kDa; b) 15 kDa; c) 50kDa

[Colour graph]

Colour reduction was lower than turbidity removal, being in the range of 59-75%. In this case, it was the 50 kDa membrane the one that presented the highest elimination values (average value of 70.3%). However, it was not very different from that observed for the other membranes (average colour elimination of 68.72%). Although the lowest MWCO membrane was expected to show the highest colour removal, the slightly higher retention exhibited by the 50 kDa membrane can be explained due to its more severe fouling during the tests.

Similar results were observed by Carbonell-Alcaina et al. (2018), who tested two organic UF membranes (5 kDa and 30 kDa) for the treatment of residual fermentation brine from the processing of table olives. These authors reported that the membrane with the highest MWCO showed the highest colour removal (around 80%), attributing it to the severe fouling exhibited by the 30 kDa membrane. Following the same analysis as for turbidity, the high removal values may also be due to the fact that most of the compounds that contributed to the colour presented higher molecular weight than the MWCO of the membranes. However, part of the coloured substances did manage to cross the membrane. They are low molecular weight solutes such as phenolic compounds. The compounds present in oil mill wastewater (including OOWW)

that give the characteristic dark colour are related to polyphenols, lignin, tannin and other high amount of minor organic compounds (Lee et al., 2019; Uğurlu et al., 2019). Therefore, coloured substances have different molecular weights and cannot be completely retained by the membrane.

For the 5 and 50 kDa membranes, colour removal was affected by both CFV and TMP, the latter variable being the one that had the greatest influence. The increase in TMP at a fixed CFV generated an increase in membrane fouling that directly influenced the percentage of colour rejection, increasing it. For the 15 kDa membrane, colour rejection was not significantly influenced by changes in TMP and CFV, being almost constant (around 66% rejection), which can be due to the lower fouling observed for this membrane as previously commented. However, for the highest TMPs tested, the increase in CFV did generate an increase in rejection.

All the three membranes showed the highest colour removal at the most extreme condition (a CFV of $4 \text{ m}\cdot\text{s}^{-1}$ and a TMP of 3 bar). This result confirms what was commented in section 3.2. Under these conditions, the membranes work above the critical flux and presented the highest fouling. The deposited particles (gel layer or cake) act as an additional layer that affects the permeation, observing a decreasing permeate flux and causing a change in selectivity (higher rejections) (Bacchin et al., 2006). In addition, as could be observed from Fig. 6, under these conditions the three membranes presented the lowest recovery of the permeate flux after rinsing; corresponding to the most severe fouling.

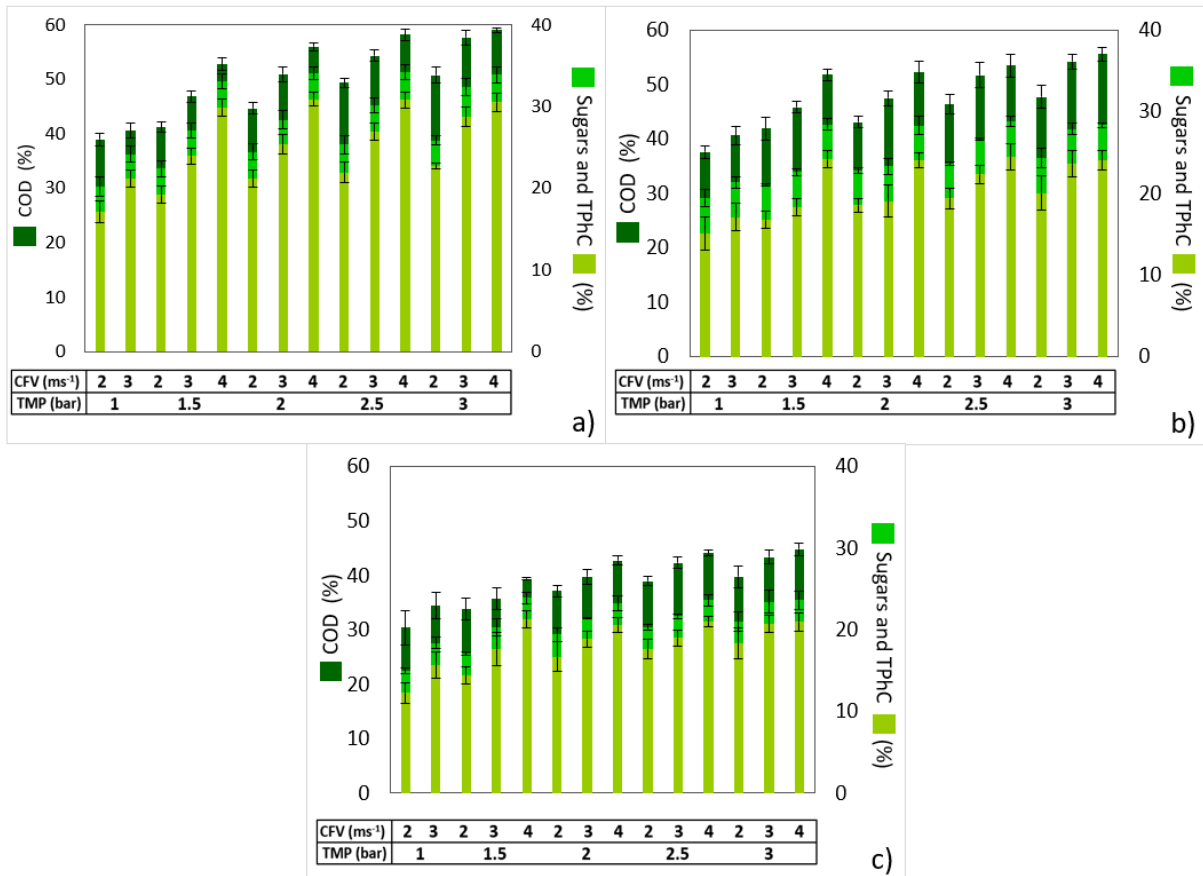


Fig. 8 COD (dark green), sugars (medium green) and Phenolic compounds (light green) rejection for the different membranes (a) 5 kDa; b) 15 kDa; c) 50kDa) and operating conditions

[Colour graph]

The membranes presented rejections between 30% and 59% of COD (Fig. 8), being the membrane with the lowest MWCO the one that presented the highest values. At 2 and 3 m·s⁻¹, a linear dependence of COD rejection with TMP was observed, achieving COD rejections between 40.9 and 57.7% for the 5kDa membrane, and between 37.6% and 54.2% for the 15 kDa one. Similar results were reported by Dafinov et al. (2005), achieving COD retentions in the range of 40-60 % when three Tami Inside ceramic membranes (including the 5 kDa and 15 kDa ones used in this study) were tested for the treatment of black liquor from wood pulping. De Almeida et al. (2018) also observed an increase in the rejection of COD with increasing TMP by different UF ceramic membranes (50 kDa and 150 kDa) in the treatment of OMW. As commented in section 3.2, it can be explained by the formation of a layer on the surface of the membrane mainly consisting of high molecular weight solutes that offer additional resistance to permeation (Turano et al., 2002). An increase in the TMP causes an increase in the gel layer thickness, thus increasing solute rejection (Baker, 1986). The highest COD rejections occurred at the highest CFV tested, as a result of the reduction of the concentration of solutes at the membrane surface as CFV increases. Moreover, as CFV increases the specific cake resistance increases, which affects

solute rejection, as it was explained in section 3.2 and observed by several authors (Foley et al., 1995; Jepsen et al., 2018). In all the analysed tests, the 50 kDa membrane was the one that presented the least influence of the operating parameters (CFV and TMP) on COD rejection. Unlike what was observed for the removal of turbidity and colour, in this case, the pore size of the membrane did influence COD rejections, being higher when the MWCO of the membrane decreased.

Rejection of phenolic compounds showed a similar trend as COD rejection, being the highest for the lowest MWCO membrane (30.9% at $4 \text{ m}\cdot\text{s}^{-1}$ and 2 bar). However, in this case the difference between the tested membranes was not so noticeable, presenting average rejections of 20% and 18% for the 15 and 50 kDa membranes, respectively. As the 50 kDa membrane has a much larger pore size than the other two membranes, a greater passage of phenols to the permeate side was expected. It is important to note that the presence of more than 30 different types of biophenols and related compounds (including tyrosol, hydroxytyrosol and oleuropein) has been found in the wastewaters from oil mills (Castro-Muñoz et al., 2019). This is due to the fact that only 2% of the phenolic compounds of the olives are found in the oily phase, leaving 98% of the remaining phenols in the wastewater (Obied et al., 2005; Rahmanian et al., 2014). Concerning their size, it has been reported that the molecular weight of the phenolic compounds present in the olives ranges between $138 - 624 \text{ g}\cdot\text{mol}^{-1}$ (Ryan and Robards, 1998); the molecular weight of the phenolic compounds present in the studied OOWW can cover a wide range.

Several factors govern the interaction between the membrane and the phenolic compounds, influencing rejection, fouling, and permeate flux. These factors include hydrophobic and hydrophilic interactions and competition between the solvent and polyphenols for the interaction sites on the membrane surface (Cassano et al., 2017). The Interaction depend on both the characteristics of the membrane and the phenolic compounds present in the sample, such as the pore size of the membrane, the molecular weight of the phenolic compounds and the electrical charge of the membrane and phenolic compounds (Sabaté et al., 2002).

The rejection is similar for all membranes due to the small size of the compounds in comparison with the MWCO of the membranes. Thus, the rejection of phenolic compounds is very low. This rejection is not 0% because of the phenolic compounds adsorption on the membrane. Although phenolic compounds could also be adsorbed by the cake layer generated during the filtration stage (Tapia-Quirós et al., 2022), sorption on the membrane structure itself cannot be ruled out. This adsorption is due to van der Waals interactions and hydrogen bonds with the hydroxyl groups of polyphenolic structures. The hydroxyl groups of phenolic compounds can form

cooperative hydrogen bonds with the hydroxyl groups on the alumina surface, resulting in more frequent and longer lasting hydrogen bonding interactions (Yeh et al., 2015)

El Rayess et al. (2012) observed a decrease in permeate flux (slight fouling) during the filtration of tannin-laden filtered wine with a 15 kDa ceramic membrane. They attributed this mainly to adsorption phenomena on the membrane, since the wine, when filtered, did not contain large particles that could form a deposit on the membrane surface. The adsorption of these components is lower on hydrophobic membranes than on hydrophilic ones. Ceramic membranes have a marked hydrophilic character and therefore the electrostatic interaction can have a significant impact on the adsorption of the phenolic compounds on the surface (Shi et al., 2021).

In this work, the membrane was positively charged (isoelectric point 6-6.9) (Live Lozada et al., 2022; Sabaté et al., 2002), while the phenolic compounds in the sample (pH 4.8) had neutral charge as their pKa value is greater than 9.0. Thus, there is no attraction between the membrane and the phenolic compounds, which facilitated their passage through the membrane and justified the low rejection presented. Similar results were observed by Harman et al. (2010) in their study of the rejection of phenol through ceramic ultrafiltration membranes at three different pH values (7.0, 10.5 and 11.5). Poor phenol rejections (3–7%) were achieved at a solution pH of 7.0. On the other hand, with increasing pH, a significant increase in phenol rejections was observed (63 and 77% of rejection at pH 10.5 and 11.5, respectively). These authors finally pointed out that these results were mainly due to electrostatic repulsion mechanisms. Since phenol is an aromatic compound with a pKa value of 9.98, at neutral or acidic pH values phenol is mainly in the neutral/undissociated form.

Considering all these comments, it can be inferred that the rejection of phenolic compounds is due to their adsorption on the surface of the membranes. On the other hand, the molecular weight of the phenolic compounds in the feed samples is lower than 15 kDa. This justifies the similar percentage of rejection obtained by 15 kDa and 50 kDa membranes, explaining, at the same time, that phenolic compounds rejection did not increase in spite of the severe fouling of the 50 kDa membrane at a CFV of $4 \text{ m}\cdot\text{s}^{-1}$. It is important to highlight that the 50 kDa membrane was the one with the highest fouling. Therefore the phenolic compounds rejection could be also explained by membrane fouling, which led to the formation of an additional barrier to the passage of some phenolic compounds (Navarro-Lisboa et al., 2017).

Although both operating parameters, CFV and TPM, were observed to affect the rejection of phenolic compounds, in this case rejection was influenced more significantly by the CFV,

increasing as this variable augmented. Phenolic compounds rejection increased linearly with the rise in TMP. However, for the highest CFV, the rejection of phenolic compounds for all the tested membranes did not show a great variation with increasing TMP. This could be explained as a result of the greatest fouling observed at these conditions, as commented in section 3.2. Again, the 50 kDa membrane was the one that presented the least variability in the rejection values when the operating conditions varied, being the highest rejection only 2% higher than the average rejection. This membrane was the one that presented the lowest rejection of phenolic compounds (12.3% at 1 bar and $2 \text{ m}\cdot\text{s}^{-1}$). Nevertheless, this low rejection was only observed under these operating conditions, then the rejection fluctuated between 17.6% and 20.9%. The 5 kDa membrane was the one with the greatest variability, presenting rejections of phenolic compounds between 17.1% and 30.8%.

On the other hand, the behaviour of the membranes against the rejection of sugars was very similar to that described for the rejection of phenolic compounds, presenting an increase in rejection with increasing both TMP and CFV. This is due to the fact that the sugars present in this water (mainly fructose, glucose, mannose and sucrose (Di Mauro et al., 2017; Rahmanian et al., 2014)) have molecular weights similar to those of some phenolic compounds. Therefore a large percentage of sugars managed to cross the membrane appearing in the permeate, which makes difficult to properly separate them from the phenolic compounds (Sánchez-Arévalo et al., 2021). The 5 kDa membrane, under the conditions of $4 \text{ m}\cdot\text{s}^{-1}$ and 2.5 bar, presented the highest rejection of sugars (34.2%), followed by the 15 kDa membrane, whose highest rejection (28.8%) was observed at the same conditions.

The best operating conditions were selected taking into account the permeate flux values, colour and turbidity removal and also the rejection of sugars, COD and phenolic compounds. A stable and high value of permeate flux is desirable, with the greatest elimination of organic matter, but without affecting the presence of phenolic compounds. These conditions were, for the 5 kDa membrane $2 \text{ m}\cdot\text{s}^{-1}$ and 2 bar, for the 15 kDa $3 \text{ m}\cdot\text{s}^{-1}$ and 3 bar, and for the 50 kDa membrane $4 \text{ m}\cdot\text{s}^{-1}$ and 2.5 bar. The phenolic compounds/COD ratio in the permeate streams at the best operating conditions selected for each membrane is presented in Fig. 9.

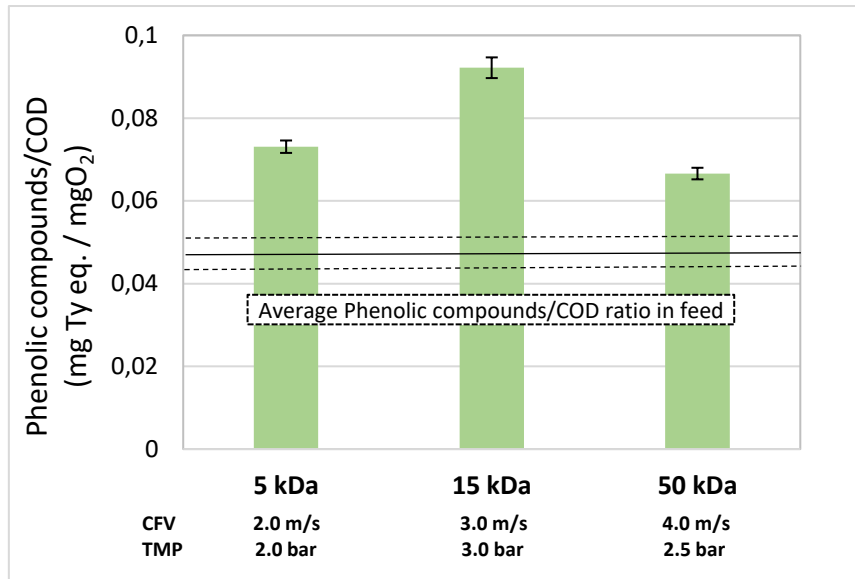


Fig. 9 Phenolic compounds/chemical oxygen demand (COD) ratio in the permeate streams for the best operating conditions for each membrane

[Colour graph]

Although the three membranes achieved an increase in the phenolic compounds/COD ratio (comparing feed and permeate streams), it was the 15 kDa membrane the one that yielded the highest increase in the ratio of phenolic compounds to COD (from 0.05 in the feed to 0.09 in the permeate), showing the greatest separation of phenolic compounds from other organic substances present in the OOWW. Cassano et al. (2011) tested different organic UF membranes with MWCOs between 4-10 kDa to treat OMW. However, they obtained similar polyphenols/total organic carbon (TOC) ratios in the feed and permeate streams. Therefore, a larger separation of phenolic compounds from other organic compounds was reached with the inorganic membranes considered in this work.

The results obtained present the 15 kDa membrane as the best option for the treatment of OOWW, achieving a partial elimination of the organic matter present in the wastewater, without significantly affecting the concentration of phenolic compounds.

3.4 Cleaning results

As previously commented, membrane fouling was observed in all the tests, being more severe for the membrane with the highest MWCO.

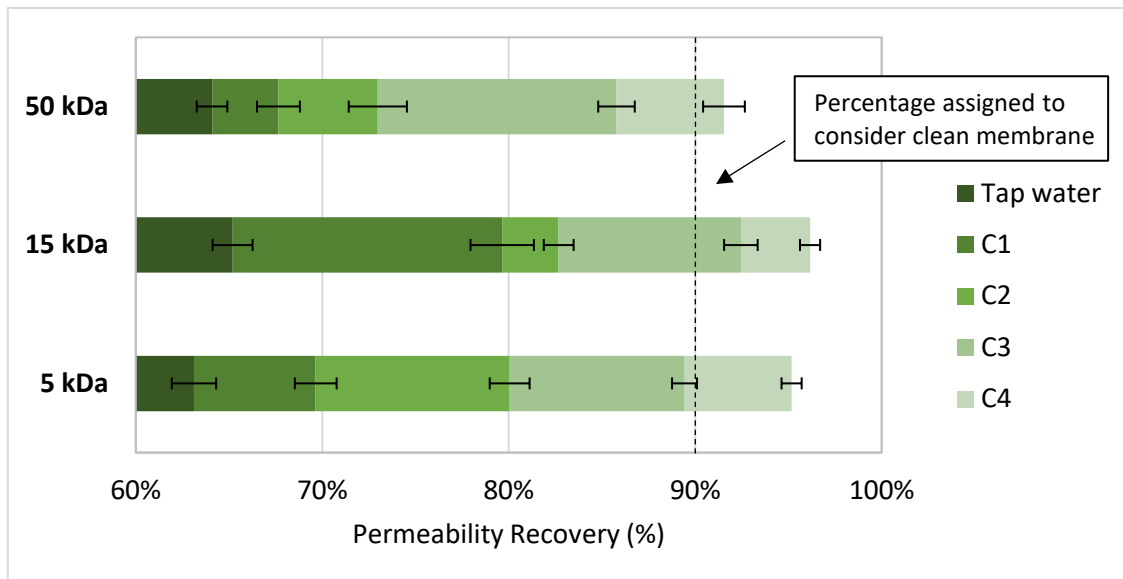


Fig. 10 Average recovery of initial pure water permeability after the different cleaning methods (rinsing with tap water; cleaning with osmotic water: C1 at 25°C and C2 at 35°C; chemical cleaning with Ultrasil 115 1%v/v: C3 at 25°C and C4 at 35°C)

[Colour graph]

Fig. 10 shows the permeability recovery of the membranes using different cleaning methods. As explained in section 2.3, firstly the membranes were rinsed with tap water and the permeability was measured immediately. Then, the different cleaning methods were successively performed, and the permeability was measured in between until all the proposed methods were completed. It was observed that the three membranes presented severe fouling, which was partially irreversible (Fig. 6). Rinsing with tap water achieved membrane permeability recoveries of around 65%. The lowest MWCO membranes showed the highest flux recovery after rinsing with tap water. Treatment C1 showed good results for the 15 kDa membrane, achieving an average permeability recovery close to 80%. However, the other two membranes reached recovery percentages below 70%. The permeability recovery after cleaning by means of C1 method for each tested operating condition can be seen in Fig. 6.

The C2 cleaning procedure improved the permeability recovery for the membrane with the lowest MWCO, which achieved 80% recovery. However, it did not represent a great change for the 15 kDa membrane, in comparison with C1 treatment. Although C2 treatment improved the permeability recovery for the 50 kDa membrane, it did not exceed 75%. In this way, cleaning with water independently of the applied temperature was not enough to recover the permeability of the membranes.

The first treatment with the chemical agent (C3) showed a great improvement in the permeability recovery for the 3 membranes. The 15 kDa membrane achieved the highest permeability recovery (93%), while the 50 kDa membrane showed the lowest recovery (86%). The increase in temperature to 35 °C (C4) implied that all the membranes could exceed the percentage assigned to consider the membrane to be clean (90%). Nevertheless, it is important to note that the 50 kDa membrane achieved the lowest recovery percentage (92%). These results were expected, since this membrane was the one that presented the greatest permeate flux decay over time in all the tests carried out, which indicates severe fouling. The nominal pore size of the membranes affects the extent and the type of fouling. It has to be highlighted that the membrane with the lowest MWCO did not yield the highest permeability recovery after cleaning, which may be due to the type of fouling that the membrane presents, which depends on the relationship between the pore size of the membranes and the size of the solutes. Corbatón-Báguena et al. (2014) studied the cleaning of several ultrafiltration membranes (including the 50 kDa Tami inside ceramic one used in this work) fouled with BSA using saline solutions. Despite the high temperatures tested, they were unable to fully recover the permeability of the 50 kDa membrane. They attributed the results to severe fouling presented by the membrane, mainly due to the penetration of BSA molecules into the porous structure of this membrane compared to smaller MWCO membranes. They explained this assumption due to the similar size of BSA and the pores of the 50 kDa membrane. Finally, it has to be pointed out that the results showed that the 15 kDa membrane was the one that presented the least irreversible fouling when the OOWW was treated under the operating conditions tested.

Nowadays, fouling remains one of the bottlenecks in the application of ceramic membranes in water treatment (Asif and Zhang, 2021). Therefore, it is essential to develop fouling prevention and control strategies to improve the hydraulic performance of the membrane. These strategies will vary depending on the wastewater. But, in general, in order to obtain higher recovery percentages, both the operational parameters of the CIP (cross flow rate, transmembrane pressure, time), as well as the pH, temperature and concentration of the chemical agent must be evaluated (Blanpain-Avet et al., 2009).

4 Conclusions

Ultrafiltration with ceramic membranes of olive oil washing wastewater has been demonstrated to be an interesting alternative as a previous step for the recovery of phenolic compounds. In order to get the best membrane performance, different CFVs and TMPs have been tested. The 50 kDa membrane, although achieved the highest permeate flux, as expected, showed a

decrease in flux as the TMP increased at a CFV of $4 \text{ m}\cdot\text{s}^{-1}$. This behaviour indicated that operation at this CFV is above the limiting conditions, presenting severe fouling. On the other hand, the other two membranes did not show significant differences in terms of rejection and permeate flux when CFV increased from 3 to $4 \text{ m}\cdot\text{s}^{-1}$. In this way, this increase is not profitable from an economic point of view.

All the three ceramic membranes tested achieved high removal of turbidity (average over 95%) and colour (average over 65%). As expected, the highest rejections were obtained for the lowest MWCO membranes, with the highest COD rejection values for the 5 kDa, 15 kDa and 50 kDa membranes being 59%, 56% and 45%, respectively. The total phenolic compounds and sugars rejection presented a similar behaviour, with the 5 kDa membrane presenting the highest rejection values for both compounds (rejection between 17.1% and 30.8% for phenolic compounds, and between 20.1% and 34.2% for sugars).

The 15 kDa membrane at the operating conditions of $3 \text{ m}\cdot\text{s}^{-1}$ and 3 bar was observed to be the best option, achieving high elimination of colour (72%), turbidity (99%) and COD (54%), without greatly affecting the concentration of phenolic compounds (rejection of 21%). A stable permeate flux of $51.4 \text{ L}\cdot\text{h}^{-1}\cdot\text{m}^{-2}$ was obtained. This membrane had the best permeability recovery under the cleaning procedures tested.

The results demonstrated that the membrane performance is conditioned by the working conditions, being affected by the interaction between the substances present in the feed and by the membrane material. This shows the importance of the selection of the appropriate membrane and operating conditions depending on the characteristics of the sample to be treated. To sum up, the ultrafiltration of OOWW using ceramic membranes seems to be a technically feasible way to remove organic matter without greatly affecting the phenolic compounds content.

Acknowledgements

The authors acknowledge the financial support from the Spanish Ministry of Economy, Industry and Competitiveness through the project CTM2017-88645-R and The European Union through the Operational Program of the Social Fund (FSE) of the Comunitat Valenciana 2014-2020.

References

Ahmed, I., Balkhair, K.S., Ahmed, A., Shaiban, J., 2017. Desalination. Chapter 10. Importance and Significance of UF / MF Membrane Systems in Desalination Water Treatment.

- APHA, 2005. Standard Methods for the Examination of Water and Wastewater, in: American Public Health Association, Washington, DC. p. 21 st. ed.
- Asif, M.B., Zhang, Z., 2021. Ceramic membrane technology for water and wastewater treatment: A critical review of performance, full-scale applications, membrane fouling and prospects. *Chem. Eng. J.* 418, 129481. <https://doi.org/10.1016/j.cej.2021.129481>
- Bacchin, P., Aimar, P., Field, R.W., 2006. Critical and sustainable fluxes: Theory, experiments and applications. *J. Memb. Sci.* 281, 42–69. <https://doi.org/10.1016/j.memsci.2006.04.014>
- Baker, R.W., 1986. Membrane Technology and Applications, third edit. ed, Chemical Age of India. John Wiley and Sons Ltd., Newark, California.
- Blanpain-Avet, P., Migdal, J.F., Bénézech, T., 2009. Chemical cleaning of a tubular ceramic microfiltration membrane fouled with a whey protein concentrate suspension- Characterization of hydraulic and chemical cleanliness. *J. Memb. Sci.* 337, 153–174. <https://doi.org/10.1016/j.memsci.2009.03.033>
- Bottino, A., Capannelli, G., Comite, A., Jezowska, A., Pagliero, M., Costa, C., Firpo, R., 2020. Treatment of olive mill wastewater through integrated pressure-driven membrane processes. *Membranes (Basel)*. 10, 1–16. <https://doi.org/10.3390/membranes10110334>
- Carbonell-Alcaina, C., Álvarez-Blanco, S., Bes-Piá, M.A., Mendoza-Roca, J.A., Pastor-Alcañiz, L., 2018. Ultrafiltration of residual fermentation brines from the production of table olives at different operating conditions. *J. Clean. Prod.* 189, 662–672. <https://doi.org/10.1016/j.jclepro.2018.04.127>
- Cassano, A., Conidi, C., Drioli, E., 2011. Comparison of the performance of UF membranes in olive mill wastewaters treatment. *Water Res.* 45, 3197–3204. <https://doi.org/10.1016/j.watres.2011.03.041>
- Cassano, A., De Luca, G., Conidi, C., Drioli, E., 2017. Effect of polyphenols-membrane interactions on the performance of membrane-based processes. A review. *Coord. Chem. Rev.* 351, 45–75. <https://doi.org/10.1016/j.ccr.2017.06.013>
- Castro-Muñoz, R., Conidi, C., Cassano, A., 2019. Recovery of Phenolic-Based Compounds From Agro-Food Wastewaters Through Pressure-Driven Membrane Technologies, Separation of Functional Molecules in Food by Membrane Technology. <https://doi.org/10.1016/b978-0-12-815056-6.00006-1>

- Çelik, G., Saygın, Ö., Balcıoğlu Akmehmet, I., 2020. Multistage recovery process of phenolic antioxidants with a focus on hydroxytyrosol from olive mill wastewater concentrates. *Sep. Purif. Technol.* 117757. <https://doi.org/10.1016/j.seppur.2020.117757>
- Cifuentes-Cabezas, M., Carbonell-Alcaina, C., Vincent-Vela, M.C., Mendoza-Roca, J.A., Álvarez-Blanco, S., 2021. Comparison of different ultrafiltration membranes as first step for the recovery of phenolic compounds from olive-oil washing wastewater. *Process Saf. Environ. Prot.* 149, 724–734. <https://doi.org/10.1016/j.psep.2021.03.035>
- Corbatón-Báguena, M.-J., Álvarez-blanco, S., Vincent-Vela, M.C., 2014. Cleaning of ultrafiltration membranes fouled with BSA by means of saline solutions. *Sep. Purif. Technol.* 125, 1–10. <https://doi.org/10.1016/j.seppur.2014.01.035>
- Corbatón-Báguena, M.J., Álvarez-Blanco, S., Vincent-Vela, M.C., 2018. Evaluation of fouling resistances during the ultrafiltration of whey model solutions. *J. Clean. Prod.* 172, 358–367. <https://doi.org/10.1016/j.jclepro.2017.10.149>
- Dafinov, A., Font, J., Garcia-Valls, R., 2005. Processing of black liquors by UF/NF ceramic membranes. *Desalination* 173, 83–90. <https://doi.org/10.1016/j.desal.2004.07.044>
- De Almeida, M.S., Martins, R.C., Quinta-Ferreira, R.M., Gando-Ferreira, L.M., 2018. Optimization of operating conditions for the valorization of olive mill wastewater using membrane processes. *Environ. Sci. Pollut. Res.* 25, 21968–21981. <https://doi.org/10.1007/s11356-018-2323-5>
- Değermenci, N., Cengiz, İ., Yildiz, E., Nuhoglu, A., 2016. Performance investigation of a jet loop membrane bioreactor for the treatment of an actual olive mill wastewater. *J. Environ. Manage.* 184, 441–447. <https://doi.org/10.1016/j.jenvman.2016.10.014>
- Dermeche, S., Nadour, M., Larroche, C., Moulti-Mati, F., Michaud, P., 2013. Olive mill wastes: Biochemical characterizations and valorization strategies. *Process Biochem.* <https://doi.org/10.1016/j.procbio.2013.07.010>
- Dhaouadi, H., Marrot, B., 2008. Olive mill wastewater treatment in a membrane bioreactor: Process feasibility and performances. *Chem. Eng. J.* 145, 225–231. <https://doi.org/10.1016/j.cej.2008.04.017>
- Di Mauro, M.D., Tomasello, B., Giardina, R.C., Dattilo, S., Mazzei, V., Sinatra, F., Caruso, M., D'Antona, N., Renis, M., 2017. Sugars and minerals enriched fraction from olive mill wastewater for promising cosmeceutical application: Characterization, in vitro and in vivo

- studies. *Food Funct.* 8. <https://doi.org/10.1039/C7FO01363A>
- Du, X., Zhang, K., Yang, H., Li, K., Liu, X., Wang, Z., Zhou, Q., Li, G., Liang, H., 2019. The relationship between size-segregated particles migration phenomenon and combined membrane fouling in ultrafiltration processes: The significance of shear stress. *J. Taiwan Inst. Chem. Eng.* 96, 45–52. <https://doi.org/10.1016/j.jtice.2018.11.016>
- El-Abbassi, A., Khayet, M., Hafidi, A., 2011. Micellar enhanced ultrafiltration process for the treatment of olive mill wastewater. *Water Res.* 45, 4522–4530. <https://doi.org/10.1016/j.watres.2011.05.044>
- El Rayess, Y., Albasi, C., Bacchin, P., Taillandier, P., Mietton-Peuchot, M., Devatine, A., 2012. Analysis of membrane fouling during cross-flow microfiltration of wine. *Innov. Food Sci. Emerg. Technol.* 16, 398–408. <https://doi.org/10.1016/j.ifset.2012.09.002>
- Foley, G., Malone, D.M., MacLoughlin, F., 1995. Modelling the effects of particle polydispersity in crossflow filtration. *J. Memb. Sci.* 99, 77–88. [https://doi.org/10.1016/0376-7388\(94\)00207-F](https://doi.org/10.1016/0376-7388(94)00207-F)
- Frolund, B., Rikke, P., Keiding, K., Nielsen, P.H., 1996. Extraction of extracellular polymers from activated sludge using a cation exchange resin. *Water Res.* 30, 1749–1758. [https://doi.org/10.1016/0043-1354\(95\)00323-1](https://doi.org/10.1016/0043-1354(95)00323-1)
- Gao, W., Liang, H., Ma, J., Han, M., Chen, Z. lin, Han, Z. shuang, Li, G. bai, 2011. Membrane fouling control in ultrafiltration technology for drinking water production: A review. *Desalination* 272, 1–8. <https://doi.org/10.1016/j.desal.2011.01.051>
- Garcia-Castello, E., Cassano, A., Criscuoli, A., Conidi, C., Drioli, E., 2010. Recovery and concentration of polyphenols from olive mill wastewaters by integrated membrane system. *Water Res.* 44, 3883–3892. <https://doi.org/10.1016/j.watres.2010.05.005>
- Garcia-Ivars, J., Durá-María, J., Moscardó-Carreño, C., Carbonell-Alcaina, C., Alcaina-Miranda, M.I., Iborra-Clar, M.I., 2017. Rejection of trace pharmaceutically active compounds present in municipal wastewaters using ceramic fine ultrafiltration membranes: Effect of feed solution pH and fouling phenomena. *Sep. Purif. Technol.* 175, 58–71. <https://doi.org/10.1016/j.seppur.2016.11.027>
- Gebreyohannes, A.Y., Mazzei, R., Giorno, L., 2016. Trends and current practices of olive mill wastewater treatment: Application of integrated membrane process and its future perspective. *Sep. Purif. Technol.* 162, 45–60.

- <https://doi.org/10.1016/j.seppur.2016.02.001>
- Harman, B.I., Koseoglu, H., Yigit, N.O., Beyhan, M., Kitis, M., 2010. The use of iron oxide-coated ceramic membranes in removing natural organic matter and phenol from waters. *Desalination* 261, 27–33. <https://doi.org/10.1016/j.desal.2010.05.052>
- He, Z., Lyu, Z., Gu, Q., Zhang, L., Wang, J., 2019. Ceramic-based membranes for water and wastewater treatment. *Colloids Surfaces A Physicochem. Eng. Asp.* 578, 123513. <https://doi.org/10.1016/j.colsurfa.2019.05.074>
- Ho, J., Sung, S., 2009. Effects of solid concentrations and cross-flow hydrodynamics on microfiltration of anaerobic sludge. *J. Memb. Sci.* 345, 142–147. <https://doi.org/10.1016/j.memsci.2009.08.047>
- Hube, S., Eskafi, M., Hrafnkelsdóttir, K.F., Bjarnadóttir, B., Bjarnadóttir, M.Á., Axelsdóttir, S., Wu, B., 2020. Direct membrane filtration for wastewater treatment and resource recovery: A review. *Sci. Total Environ.* <https://doi.org/10.1016/j.scitotenv.2019.136375>
- Jepsen, K.L., Bram, M.V., Pedersen, S., Yang, Z., 2018. Membrane fouling for produced water treatment: A review study from a process control perspective. *Water (Switzerland)* 10. <https://doi.org/10.3390/w10070847>
- Kaleh, Z., Geißen, S.U., 2016. Selective isolation of valuable biophenols from olive mill wastewater. *J. Environ. Chem. Eng.* 4, 373–384. <https://doi.org/10.1016/j.jece.2015.11.010>
- Khdair, A., Abu-Rumman, G., 2020. Sustainable environmental management and valorization options for olive mill byproducts in the Middle East and North Africa (MENA) region. *Processes* 8, 1–22. <https://doi.org/10.3390/PR8060671>
- Kujawa, J., Cerneaux, S., Kujawski, W., Bryjak, M., Kujawski, J., 2016. How to Functionalize Ceramics by Perfluoroalkylsilanes for Membrane Separation Process? Properties and Application of Hydrophobized Ceramic Membranes. *ACS Appl. Mater. Interfaces* 8, 7564–7577. <https://doi.org/10.1021/acsami.6b00140>
- Kujawa, J., Kujawski, W., Cerneaux, S., Li, G., Al-Gharabli, S., 2020. Zirconium dioxide membranes decorated by silanes based-modifiers for membrane distillation – Material chemistry approach. *J. Memb. Sci.* 596, 117597. <https://doi.org/10.1016/j.memsci.2019.117597>
- Lee, Z.S., Chin, S.Y., Lim, J.W., Witoon, T., Cheng, C.K., 2019. Treatment technologies of palm

- oil mill effluent (POME) and olive mill wastewater (OMW): A brief review. *Environ. Technol. Innov.* 15, 100377. <https://doi.org/10.1016/j.eti.2019.100377>
- Li, C., Sun, W., Lu, Z., Ao, X., Li, S., 2020. Ceramic nanocomposite membranes and membrane fouling : A review. *Water Res.* 175, 115674. <https://doi.org/10.1016/j.watres.2020.115674>
- Liu, J., Chen, K., Zou, K., He, L., Zhao, D., Wang, Z., Qiu, Y., Chen, Y., 2020. Insights into the roles of membrane pore size and feed foulant concentration in ultrafiltration membrane fouling based on collision-attachment theory. *Water Environ. Res.* 1–8. <https://doi.org/10.1002/wer.1453>
- Live Lozada, G.S., García López, A.I., Martínez-Férez, A., Ochando-Pulido, J.M., 2022. Boundary flux modelling of ceramic tubular microfiltration towards fouling control and performance maximization for olive-oil washing wastewater treatment and revalorization. *J. Environ. Chem. Eng.* 10. <https://doi.org/10.1016/j.jece.2022.107323>
- Lu, D., Zhang, T., Ma, J., 2015. Ceramic membrane fouling during ultrafiltration of oil/water emulsions: Roles played by stabilization surfactants of oil droplets. *Environ. Sci. Technol.* 49, 4235–4244. <https://doi.org/10.1021/es505572y>
- Luján-Facundo, M.J., Mendoza-Roca, J.A., Cuartas-Urbe, B., Álvarez-Blanco, S., 2016. Cleaning efficiency enhancement by ultrasounds for membranes used in dairy industries. *Ultrason. Sonochem.* 33, 18–25. <https://doi.org/10.1016/j.ultsonch.2016.04.018>
- Maaitah, M., Hodaifa, G., Malvis, A., Sánchez, S., 2020. Kinetic growth and biochemical composition variability of *Chlorella pyrenoidosa* in olive oil washing wastewater cultures enriched with urban wastewater. *J. Water Process Eng.* 35, 101197. <https://doi.org/10.1016/j.jwpe.2020.101197>
- Majewska-Nowak, K.M., 2010. Application of ceramic membranes for the separation of dye particles. *Desalination* 254, 185–191. <https://doi.org/10.1016/j.desal.2009.11.026>
- Mustafa, G., Wyns, K., Buekenhoudt, A., Meynen, V., 2016. Antifouling grafting of ceramic membranes validated in a variety of challenging wastewaters. *Water Res.* 104, 242–253. <https://doi.org/10.1016/j.watres.2016.07.057>
- Navarro-Lisboa, R., Herrera, C., Zúñiga, R.N., Enrione, J., Guzmán, F., Matiacevich, S., Astudillo-Castro, C., 2017. Quinoa proteins (*Chenopodium quinoa* Willd.) fractionated by ultrafiltration using ceramic membranes: The role of pH on physicochemical and

- conformational properties. *Food Bioprod. Process.* 102, 20–30.
<https://doi.org/10.1016/j.fbp.2016.11.005>
- Núñez Camacho, M.A., García López, A.I., Martínez-ferez, A., Ochando-Pulido, J.M., 2021. Increasing large-scale feasibility of two-phase olive-oil washing wastewater treatment and phenolic fraction recovery with novel ion exchange resins. *Chem. Eng. Process. - Process Intensif.* 164, 108416. <https://doi.org/10.1016/j.cep.2021.108416>
- Obied, H.K., Allen, M.S., Bedgood, D.R., Prenzler, P.D., Robards, K., Stockmann, R., 2005. Bioactivity and analysis of biophenols recovered from olive mill waste. *J. Agric. Food Chem.* 53, 823–837. <https://doi.org/10.1021/jf048569x>
- Ochando-Pulido, J.M., Corpas-Martínez, J.R., Martínez-Ferez, A., 2018. About two-phase olive oil washing wastewater simultaneous phenols recovery and treatment by nanofiltration. *Process Saf. Environ. Prot.* <https://doi.org/10.1016/j.psep.2017.12.005>
- Ochando-Pulido, J.M., Hodaifa, G., Victor-Ortega, M.D., Rodríguez-Vives, S., Martínez-Ferez, A., 2013. Reuse of olive mill effluents from two-phase extraction process by integrated advanced oxidation and reverse osmosis treatment. *J. Hazard. Mater.* 263P, 158–167. <https://doi.org/10.1016/j.jhazmat.2013.07.015>
- Paraskeva, C.A., Papadakis, V.G., Tsarouchi, E., Kanellopoulou, D.G., Koutsoukos, P.G., 2007. Membrane processing for olive mill wastewater fractionation. *Desalination* 213, 218–229. <https://doi.org/10.1016/j.desal.2006.04.087>
- Rahmanian, N., Jafari, S.M., Galanakis, C.M., 2014. Recovery and removal of phenolic compounds from olive mill wastewater. *J. Am. Oil Chem. Soc.* 91, 1–18. <https://doi.org/10.1007/s11746-013-2350-9>
- Ren, Q., Chen, X., Yumminaga, Y., Wang, N., Yan, W., Li, Y., Liu, L., Shi, J., 2021. Effect of operating conditions on the performance of multichannel ceramic ultrafiltration membranes for cattle wastewater treatment. *J. Water Process Eng.* 41, 102102. <https://doi.org/10.1016/j.jwpe.2021.102102>
- Roig, A., Cayuela, M.L., Sánchez-Monedero, M.A., 2006. An overview on olive mill wastes and their valorisation methods. *Waste Manag.* 26, 960–969. <https://doi.org/10.1016/j.wasman.2005.07.024>
- Roselló-Soto, E., Koubaa, M., Moubarik, A., Lopes, R.P., Saraiva, J.A., Boussetta, N., Grimi, N., Barba, F.J., 2015. Emerging opportunities for the effective valorization of wastes and by-

- products generated during olive oil production process: Non-conventional methods for the recovery of high-added value compounds. *Trends Food Sci. Technol.* 45, 296–310. <https://doi.org/10.1016/j.tifs.2015.07.003>
- Ryan, D., Robards, K., 1998. Phenolic compounds in olives. *Analyst* 123, 31–44. <https://doi.org/10.1039/a708920a>
- Sabaté, J., Pujolà, M., Llorens, J., 2002. Comparison of polysulfone and ceramic membranes for the separation of phenol in micellar-enhanced ultrafiltration. *J. Colloid Interface Sci.* 246, 157–163. <https://doi.org/10.1006/jcis.2001.8057>
- Saf, C., Villain-Gambier, M., Belaqziz, M., Ziegler-Devin, I., Trebouet, D., Ouazzani, N., 2022. Fouling control investigation by pH optimization during olive mill wastewater ultrafiltration. *Process Saf. Environ. Prot.* 164, 119–128. <https://doi.org/10.1016/j.psep.2022.06.010>
- Samaei, S.M., Gato-Trinidad, S., Altaee, A., 2018. The application of pressure-driven ceramic membrane technology for the treatment of industrial wastewaters – A review. *Sep. Purif. Technol.* 200, 198–220. <https://doi.org/10.1016/j.seppur.2018.02.041>
- Sánchez-Arévalo, C.M., Jimeno-Jiménez, Á., Carbonell-Alcaina, C., Vincent-Vela, M.C., Álvarez-Blanco, S., 2021. Effect of the operating conditions on a nanofiltration process to separate low-molecular-weight phenolic compounds from the sugars present in olive mill wastewaters. *Process Saf. Environ. Prot.* 148, 428–436. <https://doi.org/10.1016/j.psep.2020.10.002>
- Schäfer, A.I., Fane, A.G., Waite, T.D., 2000. Fouling effects on rejection in the membrane filtration of natural waters. *Desalination* 131, 215–224. [https://doi.org/10.1016/S0011-9164\(00\)90020-1](https://doi.org/10.1016/S0011-9164(00)90020-1)
- Shi, X., Zhu, L., Li, B., Liang, J., Li, X. yan, 2021. Surfactant-assisted thermal hydrolysis of waste activated sludge for improved dewaterability, organic release, and volatile fatty acid production. *Waste Manag.* 124, 339–347. <https://doi.org/10.1016/j.wasman.2021.02.024>
- Singleton, V.L., Orthofer, R., Lamuela-Raventós, R.M., 1999. Analysis of total phenols and other oxidation substrates and antioxidants by means of folin-ciocalteu reagent. *Methods Enzymol.* 299, 152–178. [https://doi.org/10.1016/S0076-6879\(99\)99017-1](https://doi.org/10.1016/S0076-6879(99)99017-1)
- Tami Industries, 2016. INSIDE CéRAM. <https://www.tami-industries.com/>
- Tapia-Quirós, P., Montenegro-Landívar, M.F., Reig, M., Vecino, X., Saurina, J., Granados, M.,

- Cortina, J.L., 2022. Integration of membrane processes for the recovery and separation of polyphenols from winery and olive mill wastes using green solvent-based processing. *J. Environ. Manage.* 307. <https://doi.org/10.1016/j.jenvman.2022.114555>
- Tomczak, W., 2013. Determination of critical flux for ultrafiltration used for separation of glycerol fermentation broths, in: Jozef, M. (Ed.), *Proceedings of the 40th International Conference of Slovak Society of Chemical Engineering*. pp. 707–714.
- Tomczak, W., Gryta, M., 2020. Application of ultrafiltration ceramic membrane for separation of oily wastewater generated by maritime transportation. *Sep. Purif. Technol.* 261, 118259. <https://doi.org/10.1016/j.seppur.2020.118259>
- Tonova, K., Lazarova, M., Dencheva-Zarkova, M., Paniovska, S., Tsibranska, I., Stanoev, V., Dzhonova, D., Genova, J., 2020. Separation of glucose, other reducing sugars and phenolics from natural extract by nanofiltration: Effect of pressure and cross-flow velocity. *Chem. Eng. Res. Des.* 162, 107–116. <https://doi.org/10.1016/j.cherd.2020.07.030>
- Turano, E., Curcio, S., De Paola, M.G., Calabrò, V., Iorio, G., 2002. An integrated centrifugation-ultrafiltration system in the treatment of olive mill wastewater. *J. Memb. Sci.* 209, 519–531. [https://doi.org/10.1016/S0376-7388\(02\)00369-1](https://doi.org/10.1016/S0376-7388(02)00369-1)
- Uğurlu, M., İlteriş Yılmaz, S., Vaizoğullar, A., 2019. Removal of Color and COD from Olive Wastewater by Using Three-Phase Three-Dimensional (3D) Electrode Reactor. *Mater. Today Proc.* 18, 1986–1995. <https://doi.org/10.1016/j.matpr.2019.06.690>
- Urbanowska, A., Kabsch-Korbutowicz, M., 2021. The use of flat ceramic membranes for purification of the liquid fraction of the digestate from municipal waste biogas plants. *Energies* 14. <https://doi.org/10.3390/en14133947>
- Waeger, F., Delhaye, T., Fuchs, W., 2010. The use of ceramic microfiltration and ultrafiltration membranes for particle removal from anaerobic digester effluents. *Sep. Purif. Technol.* 73, 271–278. <https://doi.org/10.1016/j.seppur.2010.04.013>
- Yeh, I.-C., Lenhart, J.L., Rinderspacher, B.C., n.d. Molecular Dynamics Simulations of Adsorption of Catechol and Related Phenolic Compounds to Alumina Surfaces. *J. Phys. Chem.* 2015, 7721–7731. <https://doi.org/10.1021/jp512780s>
- Žabková, M., da Silva, E.A.B., Rodrigues, A.E., 2007. Recovery of vanillin from lignin/vanillin mixture by using tubular ceramic ultrafiltration membranes. *J. Memb. Sci.* 301, 221–237.

<https://doi.org/10.1016/j.memsci.2007.06.025>